Wu et al. Advances in Bridge Engineering (2021) 2:22
https://doi.org/10.1186/s43251-021-00038-7

Advances in Bridge Engineering

ORIGINAL INNOVATION Open Access

Study on the additional support length requirements of single-span bridges due to skew using a simplified method

Suiwen Wu[1], Junfeng Jia[2], Chiyu Jiao[3*], Junfei Huang[1] and Jianzhong Li[4]

* Correspondence: jcy@bucea.edu.cn
[3]Beijing Advanced Innovation Center for Future Urban Design, Beijing University of Civil Engineering and Architecture, Beijing 100044, China
Full list of author information is available at the end of the article

Abstract

Skew bridges with seat-type abutments are frequently unseated in earthquakes due to large transverse displacements at their acute corners. It is believed these large displacements are due to in-plane rotation of the superstructure. Lack of detailed guidelines for modeling of skew bridges, many current design codes give empirical expressions rather than theoretical solutions for the additional support length required in skew bridges to prevent unseating. In this paper, a parametric study has been carried out to study the influence of skew angle, aspect ratio and fundamental periods of bridges on the additional support length requirements of single-span bridges due to skew using a shake table experiment validated Simplified Method, which is capable of simulating gap closure based on response spectrum analysis. This method is developed based on the premise that the obtuse corner of the superstructure engages the adjacent back wall during lateral loading and rotates about this corner until the loading reverses direction. A design response spectrum specified in AASHTO LRFD Specifications was employed to represent the design-level earthquakes. The results show the additional length required to prevent unseating due to skew increases with the skew angle in an approximately linear manner when the angle is less than a critical value and decreases for angles above this value. This critical skew angle increases with the aspect ratio approximately in a linear manner and shows negligible dependence on the fundamental periods of the bridges, and combination of span length and width. In addition, the critical skew angle varies between 58° and 66°, when the aspect ratio is varied from 3.0 to 5.0. The results also show that the empirical formulas for minimum support length requirements of skew bridges in current codes and specifications can not accurately reflect the influence of skew.

Keywords: Skew bridges, Simplified method, Support length requirements, Girder unseating

1 Introduction

Due to geometric and space constraints, skew bridges are commonly used as overpasses in highway interchanges or intersections, especially in urban areas. However, skew bridges with seat-type abutments are frequently unseated in earthquakes due to large transverse displacements in their acute corners (Buckle 1994; Kawashima et al. 2011; Buckle et al. 2012; Chen 2012; Kawashima 2012). For example, during the 1994 Northridge earthquake in Southern California, unseating in the acute corners was observed for the Gavin Canyon Under-crossing shown in Fig. 1, due to in-plane rotation of the superstructure (Buckle 1994). The most common explanation for this rotation is eccentricity between the centers of mass and stiffness, but this rotation has also been observed in perfectly symmetric bridges. In these cases, abutment pounding followed by rotation about one of the obtuse corners has been suggested as the unseating mechanism (Wu 2016; Wu et al. 2019a; Wu et al. 2019b).

In view of the frequent damage of the skew bridges during the past major earthquakes, intensive numerical study has been performed by a number of researchers to characterize seismic response of skew bridges, and to develop countermeasures to mitigate or eliminate the damage. The evolution of numerical modeling techniques plays an important role in understanding and prediction of seismic response of skew bridges (Ghobarah and Tso 1974; Maragakis 1985; Wakefield et al. 1991; Abdel-Mohti 2009; Maleki 2005; Meng and Lui 2002; Kaviani 2011; Kaviani et al. 2012; Shamsabadi 2007; Wu 2019a; Wu 2019b; Li et al. 2020). These techniques range from a simple beam model (Ghobarah and Tso 1974) to more sophisticated three-dimensional finite element model (Shamsabadi 2007). On the other hand, the advancement in the shake table tests has worked as a direct method to uncover the phenomena underling the complicated response of skew bridges (Kun et al. 2017; Wu et al. 2017; Wu et al. 2019a; Wu et al. 2019b).

Fig. 1 Unseating of Gavin Canyon Bridge in the 1994 Northridge Earthquake

Findings in literature have led to the increased understanding of seismic response of skew bridges, which is reflected in the following aspects. First, the unseating mechanism has been updated as follows. During the earthquake action, the skew bridges will first close the expansion gap, rotate around one of its obtuse corner and then rebound off the abutment and continue to rotate in the same direction (Buckle et al. 2012; Priestley et al. 1996; Wu 2019a). Second, seismic pounding will play an important role in seismic response of skew bridges and hence should be considered in the numerical modeling (Maragakis 1985; Maragakis and Jennings 1987; Bjornsson 1997; Shamsabadi and Kapuskar 2006; Shamsabadi 2007; Abdel-Mohti and Pekcan 2013a; Abdel-Mohti and Pekcan 2013b; Kwon and Jeong 2013; Catacoli et al. 2014; Deepu et al. 2014; Zakeri and Amiri 2014, Wu et al. 2021). Third, the friction along the contact surface of seismic collision will also play an important role in the response of skew bridges, which should not be neglected in the numerical analysis (Dimitrakopoulos 2010; Wu et al. 2019b; Wu and Buckle 2020). Furthermore, due to the significant in-plane rotation, skew bridges will subject to larger support length requirements than their straight counterparts (Jennings et al. 1971; Maragakis 1985; Buckle 1994; Mitchell et al. 1995; Bjornsson 1997; Kawashima et al. 2011; Buckle et al. 2012; Wu 2019b).

With the advancement in the numerical modeling, accurate prediction of the seismic response of skew bridges may be achievable through 3-D dynamic analysis on rigorous finite element models (Wu and Buckle 2020). However, this type of modeling technique may not be suitable for engineering practitioners during the preliminary design of bridges due to consideration of computational effort, modeling complexity and determination of the error-prone parameters in the physics-based numerical models. Given this, researchers have instead explored simplified methods to estimate the response of skew bridges. For example, a response-spectrum-analysis-based hand-method was proposed by Kalantari and Amjadian (2010) for dynamic analysis of skew highway bridges. It was found that the proposed method is able to accurately estimate the dynamic characteristics and bridge responses. However, the proposed method does not consider the seismic collision between the bridge and abutment. Therefore, its accuracy will be compromised when pounding occurs during strong earthquakes. Wu et al. (2019a) developed a simplified method to estimate the additional support length demands of bridges due to skew based on the unseating mechanism developed based on a shake table experiment, which is able to consider the bridge-abutment interaction. In that method, the seismic response of skew bridges under earthquake action is computed based on response spectrum analysis by simplifying the bridge system as a single-degree-of-freedom system. The accuracy of the developed method was also demonstrated by Wu et al. (2019a) by comparing the results with the dataset from the shake table experiment.

Even the modeling techniques of skew bridges have been improved significantly, due to the complexity in the response induced by seismic pounding, no consensus has been reached for the numerical modeling of skew bridges. As a consequence, despite the common occurrence of this type of damage, current design codes and specifications do not give explicit procedures to estimate the additional support length in skew bridges, but rely instead on empirical expressions. Without validation by rigorous numerical and experimental studies, the conservatism and non-conservatism of these empirical equations are still unknown. In this study, a comprehensive parametric study has been

carried out to investigate the additional support length requirements of single-span bridges due to skew during design-level earthquakes using the Simplified Method proposed by Wu et al. (2019a). The focus on single-span skewed bridges is in view of the frequent unseating and collapse of this type of bridges, as seen in the reconnaissance reports of recent major earthquakes, such as the 2008 Wenchuan earthquake (Chen 2012) and the 2010 Chile Maule earthquake (Buckle et al. 2012). Parameters of interest include skew angles, fundamental periods of the bridges, span length and width, and aspect ratio (span length/width). In addition, the empirical equations for the minimum additional support length requirements of bridges due to skew specified in various codes and specifications are also evaluated.

2 Simplified method

The Simplified Method used to estimate the maximum support length requirements of skew bridges was developed by Wu et al. (2019a) and had been validated by a comprehensive dataset from a shake table experiment on a family of skew bridges (Wu et al. 2019a). Details of the method and the corresponding validation process are referred to Wu et al. (2019a). Brief introduction of the method is introduced here for the readers' reference. Assumptions are made in the Simplified Method as follows.

- Rigid superstructure
- No slip along the face of abutment when the gap is closed and the back wall engaged
- Ground motion is applied in transverse direction only (y-direction in Fig. 2)
- Rigid abutment
- No transverse shear keys, and
- Rebound of superstructure away from abutment is ignored

Under these assumptions, a skew superstructure will undergo two different cases of motions during the earthquake action.

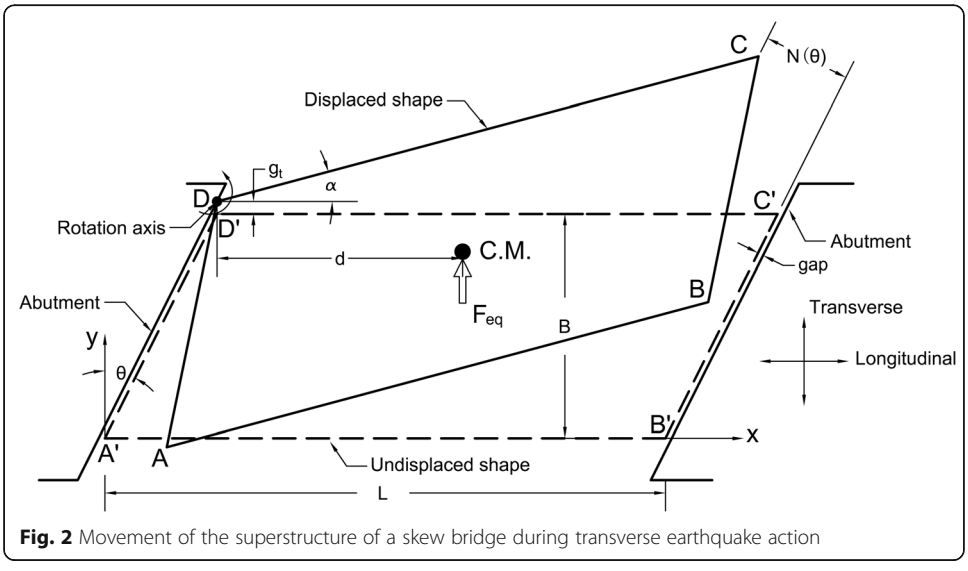

Fig. 2 Movement of the superstructure of a skew bridge during transverse earthquake action

2.1 Case 1

When the skew angle is small and the transverse gap is large (i.e. g_t in Fig. 2), under the transverse earthquake action, the displacement of the superstructure is not adequate to close the transverse gap. Hence, no gap closure and rotation of the bridge is expected in this case.

2.2 Case 2

When the skew angle is medium or large, under the transverse earthquake action, the superstructure will move transversely to close the gap and rotate around one of the obtuse corners. In this case, the acute corners at the opposite site will experience the largest support length demand (i.e. upper right corner in Fig. 2).

For both cases, the maximum support length demands of bridges due to skew $N(\theta)$ can be estimated by simplifying the bridge as a single-degree-of-freedom system (SDOF). For each case, the $N(\theta)$ (see Fig. 2) is computed based on the following procedures.

2.3 Case 1

In this case, the earthquake motion is not adequate to close the transverse gap and the bridge superstructure moves transversely. That is: $D < g_t$ where D is the transverse displacement of the center mass of the superstructure and g_t is the transverse gap (see Fig. 2). The bridge system can be simplified as a SDOF system: the mass of superstructure is supported on a series of springs representing the substructure system. Consequently, the maximum support length demand of the bridge due to skew $N(\theta)$ can be computed by response spectrum analysis and the equations are:

$$T_t = 2\pi\sqrt{m/k_1} \tag{1}$$

$$F_{eq} = mS_a \tag{2}$$

$$\Delta_y = F_{eq}/k_1 \tag{3}$$

$$N(\theta) = \Delta_y sin\theta \tag{4}$$

where T_t is the period of the bridge system in the transverse direction; m is the total mass of superstructure; k_1 is the total transverse translational stiffness of the substructure system; S_a is the acceleration response spectrum at period of T_t; F_{eq} is the equivalent maximum force applied to the superstructure; Δ_y is the displacement of the superstructure in the transverse direction and θ is the skew angle (°) as shown in Fig. 2;

2.4 Case 2

In this case, the earthquake motions are strong enough to force the superstructure to first close the gap and then rotate around one of the obtuse corners, i.e. $D > g_t$. As a result, the adjacent acute corner of the opposite site will have the largest support length demand. The transverse force-displacement relationship of the bridge system at the center mass is a bilinear curve, as shown in Fig. 3, where the first slope k_1 represents the superstructure moves transversely to close the gap while the second slope k_2 means the superstructure rotates about the obtuse corner. Since $D > g_t$, the transverse displacement of the center mass will fall within the second slope k_2. Based on this force-

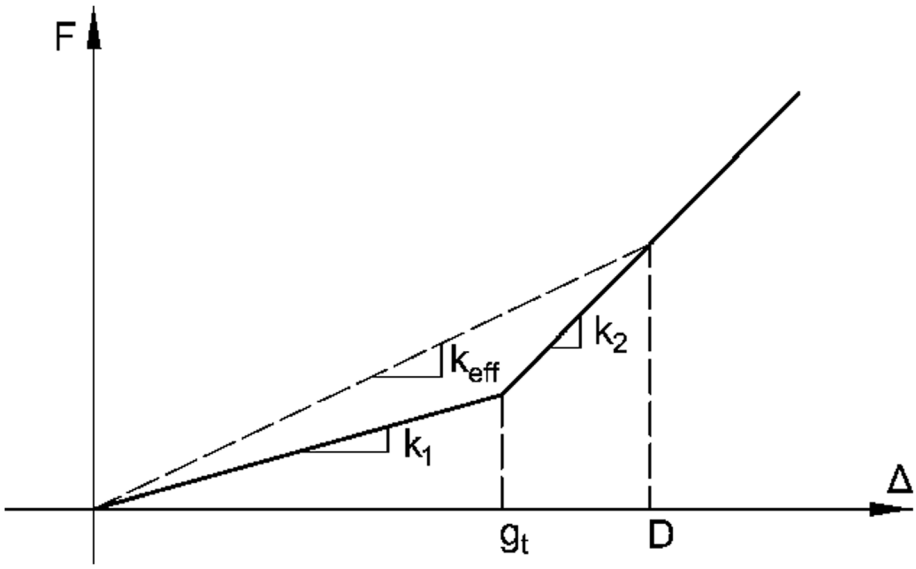

Fig. 3 Transverse force-displacement of the center of mass of a sing-span skewed bridge in case 2

displacement relationship, the bridge system can also be simplified as a SDOF system with an effective stiffness k_{eff} (see Fig. 3) to compute the maximum support length demand $N(\theta)$ of the skew bridge at the adjacent acute corner of the opposite side. With this simplification, the equations to compute $N(\theta)$ are as follows.

First, the effective period of the system can be computed by Eqs. 5, 6, 7, 8, 9 and 10.

$$k_{eff} = k_2 + (k_1 - k_2)g_t/D \tag{5}$$

$$g_t = gap/sin\theta \tag{6}$$

$$k_2 = J_d/d^2 \tag{7}$$

$$d = 0.5(L - Btan\theta) \tag{8}$$

$$J_D = \sum\left(x^2k_y + y^2k_x\right) \tag{9}$$

$$T_{eff} = 2\pi\sqrt{m/k_{eff}} \tag{10}$$

where k_2 is the equivalent transverse stiffness of the bridge when it rotates around the obtuse corner; k_{eff} is the effective transverse stiffness of the bridge system; gap is the expansion gap size normal to the abutment (see Fig. 2); J_d is the rotational stiffness of the substructure system around the obtuse corner; d is the longitudinal distance from the center of mass to the obtuse corner (see Fig. 2); L and B are the span length and width, respectively; k_x and k_y are the shear stiffness of bearings in longitudinal and transverse directions respectively and x and y are the longitudinal and transverse distances from the bearing at each corner to the obtuse corner (i.e. rotation point), respectively.

When the effective period of the system is determined, the maximum rotation angle α of the bridge is then computed based on the acceleration response spectrum. For example, for a typical design response spectrum in AASHTO LFRD (2012) as seen in Fig. 4, the α is computed in two different scenarios depending on the range value of

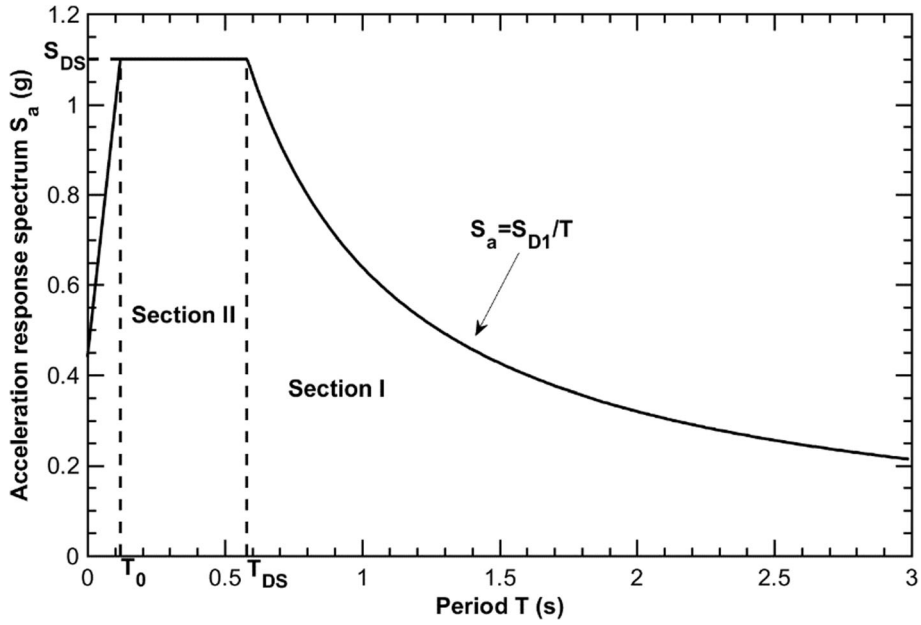

Fig. 4 Typical design response spectrum in AASHTO LRFD Specifications (2012)

T_{eff}. It is noted that the T_{eff} of single-span skew bridges will be larger than T_0 (see Fig. 4), therefore, the derivation of $N(\theta)$ in case 2 is only given for $T_{eff} > T_0$.

Assumption a: when $T_{eff} \geq T_{DS}$ (i.e. Section I in Fig. 4).

In this case, the acceleration response spectrum coefficient S_a is inversely proportional to the period of the structure and the maximum transverse displacement of the center of mass D at the effective period is:

$$D = \frac{g}{4\pi^2} S_{D1} T_{eff} \tag{11}$$

where S_{D1} is the spectral acceleration coefficient at the period of 1.0 s. Substitute Eqs. (5) and (10) into Eq. (11), and obtain:

$$4\pi^2 k_2 D^2 + 4\pi^2 (k_1 - k_2) g_t D - g^2 S_{D1}^2 m = 0 \tag{12}$$

D can be explicitly solved from Eq. (12).

Assumption b: $T_0 \leq T_{eff} < T_{DS}$ (i.e. Section II in Fig. 4).

In this case, the design acceleration response spectrum falls in the plateau and $S_a = S_{DS}$. The maximum transverse displacement of the center mass D at the effective period is:

$$D = \frac{m S_{DS} g - (k_1 - k_2) g_t}{k_2} \tag{13}$$

It is seen in Eqs. (11, 12, and 13), the maximum displacement of the center of mass D is computed based on the assumption with respect to the T_{eff}. Therefore, after the D is computed, the assumption to T_{eff} should be checked based on Eqs. (5, 6, 7, 8, 9 and 10). Then the maximum rotational angle α of the bridge is computed by:

$$\alpha = \frac{D - g_t}{d} \tag{14}$$

When the maximum rotation angle is determined, the maximum support length demands $N(\theta)$ of the bridges due to skew can be computed based on the geometry shown in Fig. 2.

$$N(\theta) = gap + (L - L\cos\alpha)\cos\theta + L\sin\alpha\sin\theta \tag{15}$$

Based on these equations, closed form solution for the maximum additional support length demand $N(\theta)$ is obtainable for the AASHTO design earthquake response spectrum.

Note that all of these procedures are for the single-span simply supported bridges. To extend the procedures to multi-span bridges, the transverse force-displacement relationship in Fig. 3 has to be updated, which is out-of-the-scope of current study.

2.5 Parametric study

It is known that parameters affecting the seismic performance of the skew bridges include skew angle, aspect ratio of superstructure (length to width ratio), soil-abutment interaction, presence of shear keys, and intensity of ground motion, and so on (Kaviani et al. 2012; Meng and Lui 2001). However, to quantify the influences of these parameters highly depends upon the robustness of the numerical models. In this section, a parametric study is carried out using the Simplified Method described above to investigate the effect of skew angle, fundamental periods of the bridges, span length and width, and the aspect ratio on additional support length demands of bridges due to skew under the design-level earthquakes. For this purpose, the design acceleration response spectrum specified in AASHTO LRFD Specifications (2012) was employed to represent the design-level earthquakes.

2.6 Prototype bridges

The seed bridge used in the parametric study is the North Yankee Slough Bridge (a typical skew bridge in California), which is a single-span simply supported box-girder bridge with span length of 35 m, width of 13.58 m and skew angle of 30°. Figure 5 shows its cross section. In order to investigate the effects of aspect ratios, span length and width, two sets of dimensions were adapted from the seed bridge. In set 1, the width was kept constant at 12.2 m, while the span was varied, and in set 2, the span (L) was kept constant at 36.6 m while the width (B) was varied. In both sets, the same aspect ratio varied from 3.0 to 5.0 as shown in Table 1. The size of expansion gap for

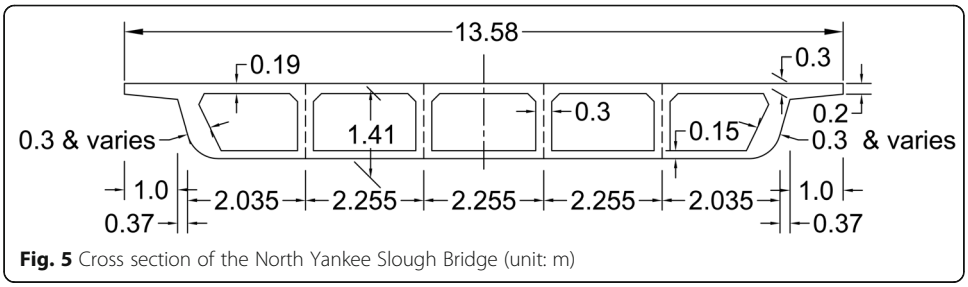

Fig. 5 Cross section of the North Yankee Slough Bridge (unit: m)

Table 1 Basic information of the prototype bridges in the parametric study

Case #	*L* (m)	*B* (m)	*L/B*	*W* (t)	# of bearings	Thermal expansion (mm)	*gap* (mm)	θ_1 (°)	θ_2 (°)
Set 1 (constant width *B* = 12.2 m)									
1	36.6	12.2	3	505	12	8.8	13	20.9	69.1
2	42.7	12.2	3.5	678	12	10.2	19	17.4	72.6
3	48.8	12.2	4	833	12	11.7	19	15.0	75.0
4	54.9	12.2	4.5	1003	12	13.2	25	13.2	76.8
5	61	12.2	5	1187	12	14.6	25	11.8	78.2
Set 2 (constant length *L* = 36.6 m)									
6	36.6	12.2	3	505	12	8.8	13	20.9	69.1
7	36.6	10.4	3.5	422	10	8.8	13	17.4	72.6
8	36.6	9.1	4	385	10	8.8	13	15.0	75.0
9	36.6	8.2	4.5	328	8	8.8	13	13.2	76.8
10	36.6	7.3	5	301	8	8.8	13	11.8	78.2

each configuration was designed based on the thermal expansion, as summarized in Table 1. For each bridge configuration, the skew angle was varied from 1 to 70°, with increments of 1° to study the skew effect.

It is assumed that all bridges are supported by elastomeric bearings and one under each web of the girder. Due to the uncertainty in the bearing stiffness, the fundamental translational period is assumed to vary from 0.7 s to 1.2 s for each configuration, a typical range for single-span, simply-supported bridges. Then the stiffness of each bearing can be back calculated by the assumed fundamental translational period based on the following equation.

$$k = \frac{4\pi^2 W}{nT^2 g} \tag{16}$$

where W is the weight of the superstructure; n is the total number of bearings; T is the fundamental translational period, g is the gravitational acceleration = $9.8\ m/s^2$.

2.7 Design response spectrum

The design response spectrum (DRS) in AASHTO LRFD Specifications (2012) was selected for the prototype bridges, which assumes a rock site (Site Class B) with a peak ground acceleration (PGA) of 0.471 g. The short-period spectral acceleration (S_s) for the site is 1.135 g, and the long-period acceleration (S_1) is 0.42 g. For Site Class B, the site factors for S_s (F_a) and S_1 (F_v) are both equal to 1.0 and thus S_{DS} and S_{D1} are computed as follows.

$$S_{DS} = F_a S_s = 1.0 \times 1.135 = 1.135 \tag{17}$$

$$S_{D1} = F_v S_1 = 1.0 \times 0.42 = 0.42 \tag{18}$$

Therefore, the bridge is located in Seismic Zone 3 ($0.3\ g < S_{D1} \le 0.50\ g$) based on the definition in Art. 3.10.6 of the AASHTO LRFD Specification (2012). The design response spectrum for the prototype bridges is plotted in Fig. 6.

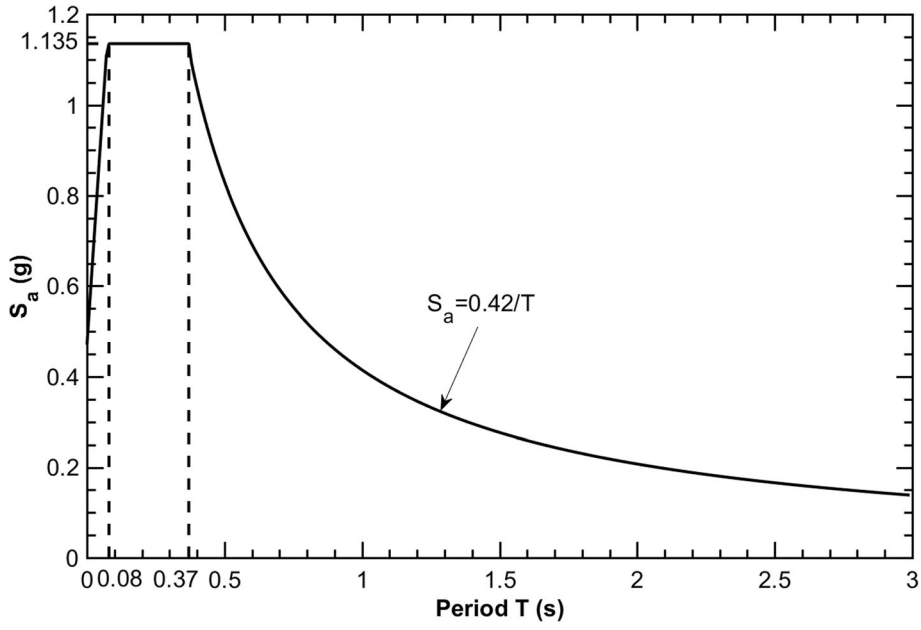

Fig. 6 Design response spectrum used in the parametric study

2.8 Analysis results

The maximum additional support length due to skew *N(θ)* of each bridge configuration with each fundamental period was estimated by the procedures of the Simplified Method (SM) described above with the design acceleration response spectrum input in the transverse direction. In this section, take the fundamental period of T = 0.9 s as a typical example. It is noted that the results of the bridges with other fundamental periods show similar trend and are not presented here for simplicity. Figure 7 plots the *N(θ)* against the skew angle *θ* for all bridge configurations with T = 0.9 s. Several observations are made in this figure.

First, for all bridge configurations, when the skew angle is very small such that the gap does not close (Motion 1), the *N(θ)* increases linearly with skew angle. When the skew angle is larger and the gap closes followed by rotation, the *N(θ)* continues to

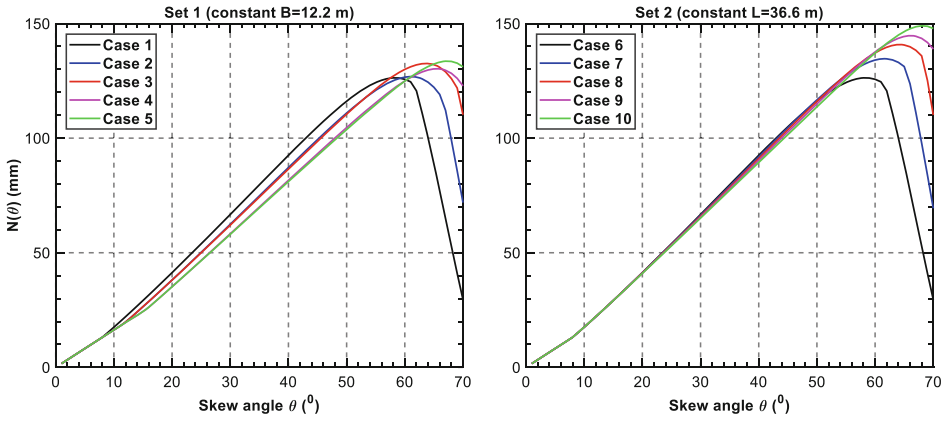

Fig. 7 Additional support length demands *N(θ)* due to skew versus skew angles (*T* = 0.9 s)

increase in a linear manner with skew angle but at a faster rate up to a specific skew angle and at a lesser rate from this angle to a critical skew angle θ_{crit}. When further increasing the skew angle to exceed the critical skew angle, the $N(\theta)$ decreases. This indicates that for each bridge configuration, there is a critical skew angle, where the additional support length due to skew is the largest among all of skew angles. Second, the critical skew angle varies with the aspect ratio of the bridge. Third, the set 1 bridges have various initial slope for the $N(\theta)$. To be specific, the cases 2 ($L/B = 3.5$) and 3 ($L/B = 4.0$) bridges have the same initial slope, while those of the cases 4 ($L/B = 4.5$) and 5 ($L/B = 5.0$) bridges are the same. In addition, all bridges in the set 2 have approximately the same initial slope. It is interesting to note that in the set 1, the cases 2 and 3 bridges have the same expansion gap size, and cases 4 and 5 bridges have the same gap size. In the set 2, all bridges have the same expansion gap size. As explained in the development of the SM, with small skew angles, the bridge will experience motion 1 without gap closure. The difference in the expansion gap size will result in different skew angles to close the gap and hence difference in the initial slope. Therefore, the observation with respect to the initial slope is due to the difference in the size of expansion gap.

The decrease of $N(\theta)$ at large skew angles shown in Fig. 7 is mainly attributed to the combination of the decrease of the eccentricity between the center of mass (C.M.) and the center of stiffness (C.S.), i.e. d in Eq. (8) and the decrease of the rotational stiffness around the center of stiffness, i.e. J_d in Eq. (9). To further explain this, take the case 1 as an example, as shown in Fig. 8. As seen in this figure, the d will decrease with skew angle. The smaller distance d will result in smaller torque T around the center of stiffness caused by the earthquake action, i.e. smaller external torque for in-plane rotation. For the rotational stiffness J_d will also decrease with the skew angle, as seen in Fig. 9a. Based on the derivation procedure of the Simplified Method, the combination of these two factors will result in increase of in-plane rotation to the critical skew angle and then decrease, as seen in Fig. 9b. As a result, the $N(\theta)$ will see the same trend based on Eq. (15).

Figure 10 plots the comparison of the $N(\theta)$ of the bridge with the same aspect ratio but with different combinations of the L and B. It is clearly seen that even with the same aspect ratio, the bridges in the sets 1 and 2 still show difference in the $N(\theta)$. This indicates that the $N(\theta)$ will be affected by the aspect ratio as well as the combinations of the L and B.

Figure 11 plots the comparison of the $N(\theta)$ of the bridges with the same aspect ratio of 4.0 in both sets 1 and 2 but with different fundamental periods. It is seen that the same skew angle, the $N(\theta)$ always increases with the fundamental period of the bridge,

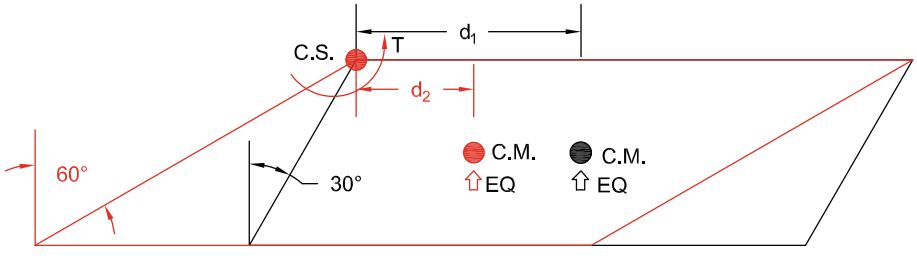

Fig. 8 Illustration of the eccentricity between the center of mass and center of stiffness d with different skew angles ($T = 0.9$ s)

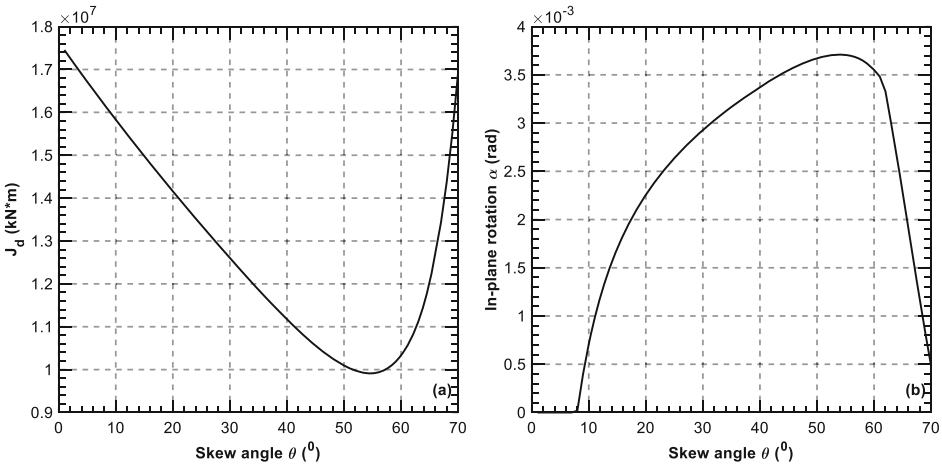

Fig. 9 Parameter and response of the case 1 ($L = 36.6$ m, $B = 12.2$ m and $L/B = 3.0$). **a** Rotational stiffness J_d; **b** computed in-plan rotation from the Simplified Method ($T = 0.9$ s)

regardless of the bridge in the sets 1 and 2. This indicates that the factor influencing the $N(\theta)$ should also include the fundamental period T.

As noted in Fig. 7, for each bridge configuration, there is a critical skew angle θ_{crit} where the largest $N(\theta)$ occurs. Figure 12 shows the critical skew angle versus the aspect ratio L/B for bridges with different fundamental periods. As seen in Fig. 12, for each fundamental period, the θ_{crit} increases with the aspect ratio approximately in a linear manner, for both sets of bridges. In addition, the θ_{crit} has slight difference when the fundamental period varies from 0.7 s to 1.2 s. The largest difference is about 3°. Therefore, the fundamental period has negligible influence on the critical skew angle. Moreover, for the same aspect ratio, the critical skew angles of the bridges in sets 1 and 2

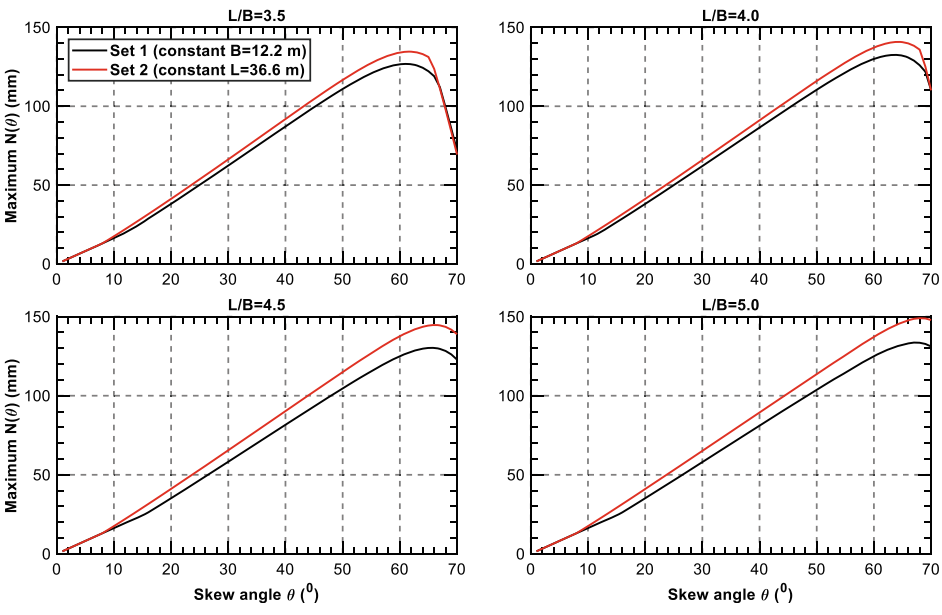

Fig. 10 Comparison of the maximum additional support length demand due to skew $N(\theta)$ for prototype bridges with the same aspect ratio but different combinations of L and B ($T = 0.9$ s)

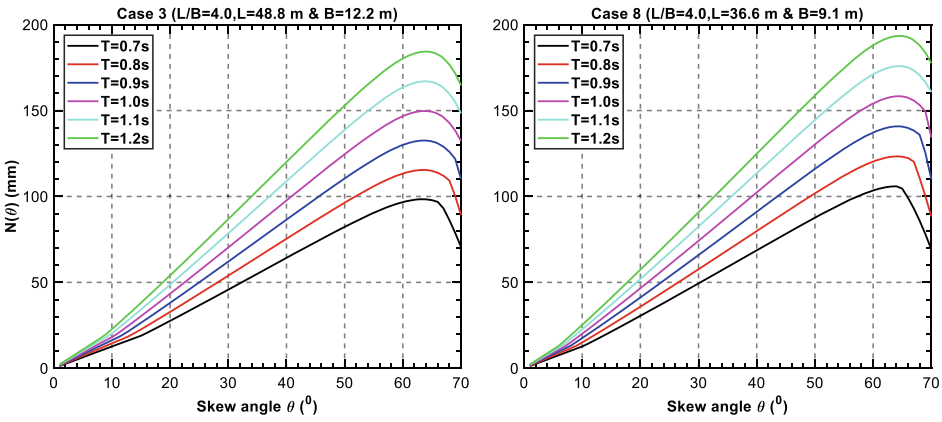

Fig. 11 Comparison of the maximum additional support length demand due to skew *N(θ)* for prototype bridges with aspect ratio of 4.0 and different fundamental periods

agree well with each other, indicating that the critical skew angle is mainly dependent upon the aspect ratio of the bridge while has negligible dependence on the combination of L and B.

Since the critical skew angle is insensitive to the fundamental periods and combination of L and B, while shows approximately linear dependence on the aspect ratio, linear regression analysis is then performed on the computed critical skew angles of the two sets of bridges, as shown in Fig. 13. The results indicate that the critical skew angle is related with the aspect ratio in the following equation.

$$\theta_{crit} = 5.88\left(\frac{L}{B}\right) + 39.5^0 \tag{19}$$

2.9 *N(θ)* in current codes and specifications

In this section, the additional support length due to skew *N(θ)* specified current codes and specifications are reviewed, including AASHTO LRFD Specifications (2012), AASH TO Guide Specitifications, (2011) FHWA Seismic Retrofitting Manual for Highway

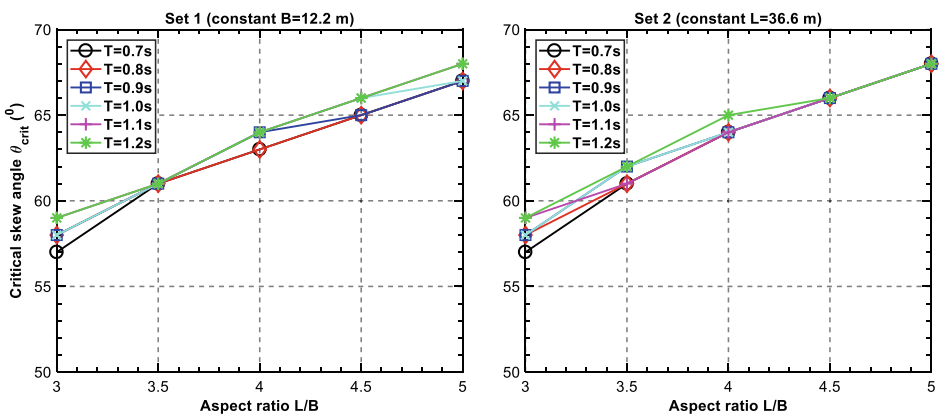

Fig. 12 Critical skew angle versus aspect ratio

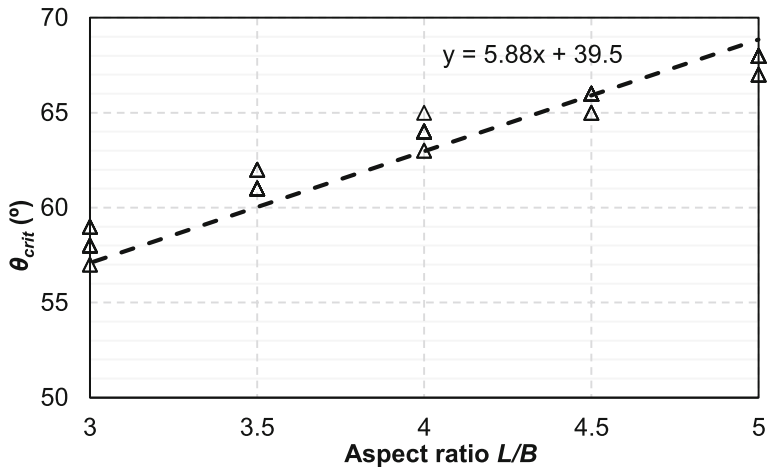

Fig. 13 Regression of critical skew angles

Structures (Buckle et al. 2006) and China Specifications for Seismic Design of Highway Bridges (JTG/T 2231-01-2020 2020). The *N(θ)* is defined by

$$N(\theta) = N_\theta - N_0 \tag{20}$$

where N_θ and N_0 are the minimum support length requirements of skew bridges and straight bridges, respectively.

2.10 AASHTO LRFD (2012) and AASHTO Guide Specifications (2011)

It is specified in AASHTO LRFD (2012) and AASHTO Guide Specifications (2011) and that without restrainers, shock transmission units, or dampers at the expansion bearings, the minimum support length for skew bridges N_θ located in Seismic Zone 3 should satisfy the empirical Eq. (21).

$$\begin{aligned} N_\theta &= 1.5 \times (203 + 0.155L + 0.619H)\left(1 + 0.000125\theta^2\right) \\ &= N_0\left(1 + 0.000125\theta^2\right) \end{aligned} \tag{21}$$

where H is the average height of the column and for single span bridge, is equal to 0. The unit in this formula is mm for N_θ and N_0, m for L and degree for θ. Then based on the definition of *N(θ)* in Eq. (20), it can be computed by:

$$\begin{aligned} N(\theta) = N_\theta - N_0 &= 1.5 \times (203 + 0.155L + 0.619H)\left(0.000125\theta^2\right) \\ &= N_0 0.000125\theta^2 \end{aligned} \tag{22}$$

It can be seen clearly from the Eq. (22) that the *N(θ)* increases with the skew angle in a parabolic way.

2.11 FHWA seismic retrofit manual for highway structures (Buckle et al. 2006)

In FHWA's report by Buckle et al. (2006), the support length of existed skew bridges should check:

$$N_\theta = \left[102 + 0.155L + 0.619H + 15.43\sqrt{H}\sqrt{1 + \left(\frac{2B}{L}\right)^2}\right]\frac{(1 + 1.25F_vS_1)}{cos\theta} = \frac{N_0}{cos\theta} \tag{23}$$

where L is the distance between joints (m); B is span width (m); H is the tallest pier between the joints (m), F_v is site coefficient for the long-period range; and S_1 is response spectral acceleration coefficient at 1.0 s. $N(\theta)$ calculated from Eq. (23) is in unit of mm. It is noted that the ratio of B/L in Eq. (23) needs to be taken greater than 3/8. Then $N(\theta)$ is computed as follow.

$$N(\theta) = N_\theta - N_0 = \frac{N_0(1 - cos\theta)}{cos\theta} \tag{24}$$

2.12 China specifications for seismic Design of Highway Bridges (JTG/T 2231-01-2020, 2020)

In the China Specifications for Seismic Design Highway Bridges (2020), for straight bridges, the support length should be the larger of the values computed by Eq. (25) or 600 mm. While for a skew bridge with superstructure geometry satisfying Eq. (26), the support length shall be the larger value of Eqs. (25) and (27) and 600 mm.

$$N_0 = 500 + L + 8H + 5L_k \tag{25}$$

$$sin2\theta \geq 2B/L_\theta \tag{26}$$

$$N_\theta = 500L_\theta(cos\theta - cos(\theta + \alpha_E)) \tag{27}$$

where L and L_θ are both the total length of the bridge (m); B is the span width (m); L_k is the maximum span length of a continuous bridge (m); and H is the average height of columns within a continuous span. The unit is mm for N_θ and N_0. It is very interesting to note that the minimum support length of skew bridges are dependent on the aspect ratio (B/L) of superstructure and the relative values between Eq. (25) and (27). The additional support length due to skew are then computed base on Eq. (20). In fact, the Eq. (26) determines a limit range for skew angle as the following.

$$\theta_1 = \frac{1}{2}\arcsin\frac{2B}{L_\theta} \leq \theta \leq \frac{\pi}{2} - \frac{1}{2}\arcsin\frac{2B}{L_\theta} = \theta_2 \tag{28}$$

Beyond this skew angle range, the N_θ is equal to N_0 and hence $N(\theta)$ is equal to zero. Within this range, the $N(\theta)$ could also be equal to zero depending upon the relative values of N_θ and N_0. It is noted that this skew angle range is only dependent on the aspect ratio. For each bridge configuration, the skew angle range is computed and summarized in Table 1.

2.13 Comparison of the $N(\theta)$

The additional support length due to skew $N(\theta)$ for each bridge configuration computed by the Simplified Method are compared with the empirical formula specified in various codes and specifications as described above. In this section, take the bridge with aspect ratio of 4.0 and T = 0.9 s as a typical example. Figure 14 shows the comparison of $N(\theta)$ for the bridge of aspect ratio of 4.0 with T = 0.9 s between the SM and current

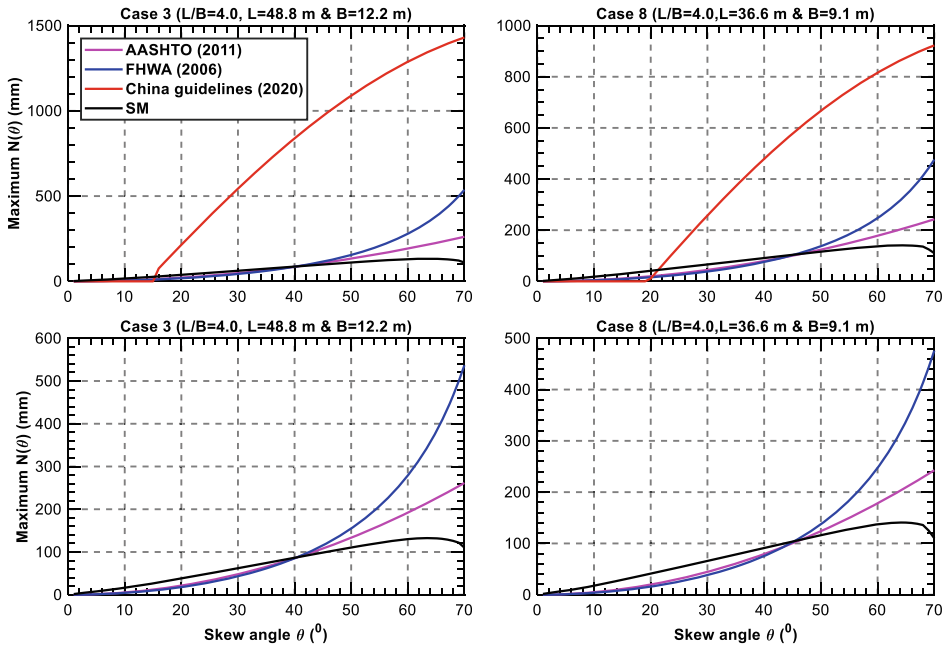

Fig. 14 Comparison of the additional support length *N(θ)* for prototype bridges of aspect ratio of 4.0 between various code specifications and the Simplified Method ($T = 0.9$ s)

codes and specifications. Note that the comparison for other bridge configurations shows similar trend and the results are not shown here for simplicity.

There are several observations in Fig. 14. First, for the same bridge model, the FHWA (2006) shows similar results with the AASHTO (2011) when the skew angle changes from 0° to 40° for the case 3 bridge and from 0° to 45° for the case 8 bridge, and both codes give smaller results than the Simplified Method. When further increasing the skew angle, both codes start to yield larger *N(θ)* in a faster rate. For example, when the skew angle is 60°, the *N(θ)* is 178 mm and 247 mm for FHWA (2006) and AASHTO (2011), respectively, which is 30% and 80% larger than the SM (137 mm), respectively. This clearly indicates that both the FHWA and AASHTO specifications could significantly underestimate the *N(θ)* when the skew angle varies from 0° to a specific value, while could significantly overestimate the *N(θ)* beyond this specific skew angle. This specific skew angle for the turning point of underestimation and overestimation for these two codes depends upon the combination of span length and width. In addition, for the case 3 bridge, the China Guidelines (JTG/T 2231-01-2020 2020) gives 0 for *N(θ)* when the skew angle is between 0° and 19°, indicating no skew effect is expected during this skew angle range. This clearly is a significant underestimation of the skew effect. The reasons for this observation are twofold. First, based on Eq. (28), when the skew angle is between 0° and θ_1, (i.e. 15°), the N_θ is specified to be equal to N_0 and hence *N(θ)* is equal to zero. Second, when the skew angle is 15° and 19°, the N_θ in Eq. (27) is smaller than N_0 in Eq. (25) and hence N_θ is equal N_0, resulting in zero for the *N(θ)*. When the skew angle increases from 19° to 70°, the *N(θ)* increases with the skew angle in a fast rate. This leads to underestimation of *N(θ)* for skew angle is between 19° and 21°, and significant overestimation for skew angle between 21° and 70°. For example, when the skew angle is 40°, the *N(θ)* from the China Guidelines is equal to 645

mm, which is 6.5 times larger than the value of the SM (86 mm). Similar observation is made for the comparison for the case 8 bridge between the SM and the China Guidelines. Therefore, the China guidelines could significantly underestimate the effect of skew on the support length requirements when the skew angle is small, while could significantly overestimate the support length requirements when the skew angle is in the medium to large range. Above all, none of the empirical formulas for the support length requirements of skew bridges in current codes and specifications can accurately reflect the influence of skew on the support length requirements.

3 Conclusions

In this paper, a comprehensive parameter study was carried out using a shake table experiment validated Simplified Method to investigate the influence of skew angles, superstructure aspect ratio (span length/span width), fundamental periods of the bridges and combinations of the span length and width on the additional support length requirements of bridges due to skew. This method is developed to estimate the additional support length requirements of bridges due to skew based on the premise that the obtuse corner of the superstructure engages the back wall of the abutment during lateral loading and the superstructure then rotates about this corner. Parameters of interests include skew angles, fundamental periods of the bridges, aspect ratio, and combination of span length and width. To be specific, two sets of prototype bridges were used which had the same set of aspect ratios from 3.0 to 5.0, with increments of 0.5, but different combinations of the span length and width. For each bridge, the bearing properties were varied to give the fundamental period changing from 0.7 s to 1.2 s to represent the uncertainty in the bridge dynamic properties, and the skew angle was varied from 0° to 70°, a typical range for practical bridges. A design response spectrum defined in AASHTO LRFD was used to represent the design-level earthquakes in Seismic Zone 3, and to excite the prototype bridges. The results for the additional support length due to skew was also compared with empirical formulas specified in current codes and specifications. General findings from this study are as follows.

- The additional length required to prevent unseating due to skew $N(\theta)$, increases with the skew angle in an approximately linear manner when the angle is between 0° and a critical skew angle θ_{crit} and then decreases with the skew angle.
- The θ_{crit} increases with the aspect ratio approximately in a linear manner and shows negligible dependence upon the fundamental periods of the bridges and combination of the span length and width. The θ_{crit} is in the range of 58° to 66°, when the aspect ratio is varied from 3.0 to 5.0. The θ_{crit} is related with the aspect ratio by:

$$\theta_{crit} = 5.88\left(\frac{L}{B}\right) + 39.5^0$$

- The $N(\theta)$ is also a function of the combination of span length and width. The bridge with the same aspect ratio but different combinations of L and B could have different $N(\theta)$.

- The results from the Simplified Method suggest that the empirical equations for minimum support length of skew bridges in the AASHTO LRFD Specifications (2012) and AASHTO Guide Specifications for Seismic Design of Bridges (2011), the FWHA Seismic Retrofitting Manual for Highway Structures (2006) and the China Specifications for Seismic Design of Highway Bridges (2020), could significantly underestimate the effect of skew on support length when the skew angle varies from zero to a specific value while could significantly overestimate the effect of skew beyond this specific angle. The specific angle depends upon the aspect ratio and the combination of the span length and width. Therefore, the empirical formulas for minimum support length requirements of skew bridges in current codes and specifications can not accurately reflect the influence of skew.

Abbreviations
SDOF: Single-degree-of-freedom; SM: Simplified Method; DRS: Design response spectrum

Acknowledgements
Not Applicable.

Authors' contributions
SW drafted the manuscript and performed the parametric study, JJ processed the data, prepared the plots, and assisted in draft preparation, CJ provided guidance in methodology development, data interpretation and technical writing, JH carried out the analytical study and substantially revised the draft, and JL participated in the design of the study and interpretation of data. The authors read and approved the final manuscript.

Funding
This research is jointly funded by the National Natural Science Foundation of China under the grant No. 52078023, the National Key Laboratory of Civil Engineering Disaster Relief Fund under grant No. SLDRCE-14-02, and the Fundamental Research Funds for Beijing University of Civil Engineering and Architecture under the grant No. X20094 and X18303.

Availability of data and materials
All data generated or analyzed during this study are included in this published article.

Declarations

Competing interests
The authors declare that they have no competing interests.

Author details
[1]Department Civil and Environmental Engineering, University of Nevada, Reno, NV 89557, USA. [2]Key Laboratory of Urban Security and Disaster Engineering of Ministry of Education, Beijing University of Technology, Beijing 100124, China. [3]Beijing Advanced Innovation Center for Future Urban Design, Beijing University of Civil Engineering and Architecture, Beijing 100044, China. [4]State Key Laboratory of Disaster Reduction in Civil Engineering, Tongji University, Shanghai 200092, China.

Received: 22 December 2020 Accepted: 4 March 2021
Published online: 28 May 2021

References
AASHTO (2011) Guide specifications for LRFD seismic bridge design. American Association of State Highway and Transportation Officials, Washington, D.C.
AASHTO (2012) AASHTO LRFD bridge design specifications, 6th edn. American Association of State Highway and Transportation Officials, Washington, D.C.
Abdel-Mohti A (2009) Seismic response assessment and recommendations for the design of skewed highway bridges. Doctoral Thesis, University of Nevada, Reno
Abdel-Mohti A, Pekcan G (2013a) Effect of skew on the seismic vulnerability of RC box girder highway bridges. Int J Stabil Struct Dynam 13(6):1350013. https://doi.org/10.1142/S0219455413500132
Abdel-Mohti A, Pekcan G (2013b) Assessment of seismic performance of skew reinforced concrete box girder bridges. Int J Adv Struct Eng 5(1):1. https://doi.org/10.1186/2008-6695-5-1
Bjornsson S (1997) Seismic response of skew bridges. Doctoral Dissertation, University of Washington, Seattle
Buckle IG, Friedland I, Mander J, Martin G, Nutt R, Power M (2006) Seismic retrofitting manual for highway structures part 1-bridges. Report No. FHWAHRT-06-032, Federal Highway Administration.
Buckle IG (1994) The Northridge California earthquake of January 17, 1994: performance of highway bridges. NCEER-94-0008, National Center for Earthquake Engineering Research, Buffalo

Buckle IG, Hube M, Chen G, Yen W-H, Arias J (2012) Structural performance of bridges in the offshore Maule earthquake of 27 February, 2010. Earthquake Spectra 28(1):533–552. https://doi.org/10.1193/1.4000031
Catacoli SS, Ventura CE, Finn WDL, Taiebat M (2014) In-plane rotational demands of skewed bridges due to earthquake induced pounding. Proc. 10th National Conference Earthquake Engineering, Earthquake Engineering Research Institute, Anchorage
Chen L (2012) Report on highway damage in the Wenchuan earthquake. China Communication Press
Deepu SP, Prajapat K, Ray-Chaudhuri S (2014) Seismic vulnerability of skew bridges under bi-directional ground motions. Eng Struct 71:150–160. https://doi.org/10.1016/j.engstruct.2014.04.013
Dimitrakopoulos EG (2010) Analysis of a frictional oblique impact observed in skew bridges. Nonlinear Dynam 60(4):575–595. https://doi.org/10.1007/s11071-009-9616-7
Ghobarah AA, Tso WK (1974) Seismic analysis of skewed highway bridges with intermediate supports. Earthq Eng Struct Dyn 2:235–248
Jennings PC, Housner GW, Hudson DE, Trifunac MD, Frazier GA, Wood JH, et al (1971). Engineering features of the San Fernando earthquake of February 9, 1971. Report no. EERL 71-02. Earthquake Engineering Research Laboratory, California Institute of Technology, Pasadena, CA.
JTG/T 2231–01-2020 (2020) Specifications for seismic Design of Highway Bridges. Ministry of Transport of the People's Republic of China, Beijing In Chinese
Kalantari A, Amjadian M (2010) An approximate method for dynamic analysis of skewed highway bridges with continuous rigid deck. Eng Struct 32(9):2850–2860. https://doi.org/10.1016/j.engstruct.2010.05.004
Kaviani P (2011) Performance-based seismic assessment of skewed bridges. Doctoral Dissertation, Department of Civil and Environmental Engineering, University of California, Irvine
Kaviani P, Zareian F, Taciroglu E (2012) Seismic behavior of reinforced concrete bridges with skew-angled seat-type abutments. Eng Struct 45:137–150. https://doi.org/10.1016/j.engstruct.2012.06.013
Kawashima K (2012) Damage of bridges due to the 2011 Great East Japan Earthquake. Proceedings of the International Symposium Engineering Lessons Learned from 2011 Great East Japan Earthquake, Tokyo, Japan, 82–101.
Kawashima K, Unjoh S, Hoshikuma JI, Kosa K (2011) Damage of bridges due to the 2010 Maule Chile earthquake. J Earthq Eng 15(7):1036–1068. https://doi.org/10.1080/13632469.2011.575531
Kun C, Jiang L, Chouw N (2017) Influence of pounding and skew angle on seismic response of bridges. Eng Struct 148:890–906. https://doi.org/10.1016/j.engstruct.2017.07.024
Kwon OS, Jeong SH (2013) Seismic displacement demands on skewed bridge decks supported on elastomeric bearings. J Earthq Eng 17(7):998–1022. https://doi.org/10.1080/13632469.2013.791894
Li S, Xiang P, Wei B, Lu Y, Ye X (2020) A nonlinear static procedure for the seismic design of symmetrical irregular bridges. Shock Vib. https://doi.org/10.1155/2020/8899705
Maleki S (2005) Seismic modeling of skewed bridges with elastomeric bearings and side retainers. J Bridg Eng 10(4):442–449. https://doi.org/10.1061/(ASCE)1084-0702(2005)10:4(442)
Maragakis EA (1985) A model for the rigid body motions of skew bridges. Doctoral Dissertation, Caltech, Pasadena
Maragakis EA, Jennings PC (1987) Analytical models for the rigid body motion of skew bridges. Earthq Eng Struct Dyn 15(8):923–944. https://doi.org/10.1002/eqe.4290150802
Meng JY, Lui EM (2001) Dynamic response of skew highway bridges. J Earthq Eng 5(3):205–223. https://doi.org/10.1080/13632460109350392
Meng JY, Lui EM (2002) Refined stick model for dynamic analysis of skew highway bridges. J Bridg Eng 7(3):1–11
Mitchell D, Bruneau M, Williams M, Anderson D, Saatcioglu M, Sexsmith R (1995) Performance of bridges in the 1994 Northridge earthquake. Can J Civ Eng 22(2):415–427. https://doi.org/10.1139/l95-050 Ottawa, Canada
Priestley MJN, Calvi GM, Seible F (1996) Seismic design and retrofit of bridges. John Wiley & Sons, New York, USA.
Shamsabadi A (2007) Three-dimensional nonlinear seismic soil-abutment-foundation structure interaction analyses of skewed bridges. Doctoral Dissertation, Department of Civil and Environmental Engineering, University of Southern California (USC), Los Angeles
Shamsabadi A, Kapuskar M (2006) Nonlinear seismic soil-abutment-structure interaction analysis of skewed bridges. 22th US - Japan Bridge Engineering Workshop, Seattle
Wakefield RR, Nazmy AS, Billington DP (1991) Analysis of seismic failure in skew RC bridge. J Struct Eng 117(3):972–986. https://doi.org/10.1061/(ASCE)0733-9445(1991)117:3(972)
Wu S (2016) Effect of skew on seismic performance of bridges with seat-type abutments. Doctoral thesis, Department of Civil and Environmental Engineering, University of Nevada, Reno
Wu S (2019a) Unseating mechanism of a skew bridge with seat-type abutments and a simplified method for estimating its support length requirement. Eng Struct 191:194–205. https://doi.org/10.1016/j.engstruct.2019.04.059
Wu S (2019b) Investigation on the connection forces of shear keys in skew bridges during earthquakes. Eng Struct 194:334–343. https://doi.org/10.1016/j.engstruct.2019.05.020
Wu S, Buckle IG (2020) Effect of skew on the minimum support length requirements of single-span bridges with seat-type abutments. Earthquake Spectra 36(3):1119–1140. https://doi.org/10.1177/8755293020919427
Wu S, Buckle IG, Itani AM (2017) Experimental and analytical study of girder unseating in skewed bridges during earthquakes. 16th World Conference on Earthquake Engineering, Santiago
Wu S, Buckle IG, Itani AM, Istrati D (2019a) Experimental studies on seismic response of skew bridges with seat-type abutments. I: shake table experiments. J Bridg Eng 24(10):04019096. https://doi.org/10.1061/(ASCE)BE.1943-5592.0001480
Wu S, Buckle IG, Itani AM, Istrati D (2019b) Experimental studies on seismic response of skew bridges with seat-type abutments. II: results. J Bridg Eng 24(10):04019097. https://doi.org/10.1061/(ASCE)BE.1943-5592.0001469
Wu S, Huang J, Li W, Jiao C, Li J (2021) Unseating of single-span bridges with skew angles out of the limit range for free rotation. Structures 32:1320–1330
Zakeri B, Amiri GG (2014) Probabilistic performance assessment of retrofitted skewed multi-span continuous concrete I-girder bridges. J Earthq Eng 18(6):945–963. https://doi.org/10.1080/13632469.2014.916241

Publisher's Note